

MKPH-T-07-15

Relativistic corrections to the static potential at $O(1/m)$ and $O(1/m^2)$

Yoshiaki Koma*

Numazu College of Technology, Numazu 410-8501, Japan

E-mail: koma@numazu-ct.ac.jp

Miho Koma†

Institut für Kernphysik, Johannes Gutenberg-Universität Mainz, D-55099 Mainz, Germany

E-mail: mkoma@kph.uni-mainz.de

Hartmut Wittig

Institut für Kernphysik, Johannes Gutenberg-Universität Mainz, D-55099 Mainz, Germany

E-mail: wittig@kph.uni-mainz.de

We investigate the relativistic corrections to the static potential, i.e. the $O(1/m)$ potential and the $O(1/m^2)$ velocity-dependent potentials, in SU(3) lattice gauge theory. They are important ingredients of potential nonrelativistic QCD for heavy quarkonium. Utilizing the multi-level algorithm, we obtain remarkably clean signals of these potentials up to $r = 0.9$ fm. We observe long range nonperturbative contributions to these corrections.

The XXV International Symposium on Lattice Field Theory

July 30 - August 4 2007

Regensburg, Germany

*Speaker of “Determination of the velocity-dependent potentials at $O(1/m^2)$ ”

†Speaker of “Relativistic correction to the static potential at $O(1/m)$ ”

1. Introduction

A possible strategy of studying heavy quarkonium in QCD is to employ potential nonrelativistic QCD (pNRQCD) [1, 2, 3, 4], which is obtained by integrating out the scale above the heavy quark mass $m \gg \Lambda_{\text{QCD}}$ and the scale mv , where v is quark velocity. The effective hamiltonian of pNRQCD up to $O(1/m^2)$ [3] is then given by

$$H = \frac{\vec{p}_1^2}{2m_1} + \frac{\vec{p}_2^2}{2m_2} + V^{(0)}(r) + \frac{1}{m_1}V^{(1,0)}(r) + \frac{1}{m_2}V^{(0,1)}(r) + \frac{1}{m_1^2}V^{(2,0)}(r) + \frac{1}{m_2^2}V^{(0,2)}(r) + \frac{1}{m_1m_2}V^{(1,1)}(r) + O(1/m^3), \quad (1.1)$$

where m_1 and m_2 denote the masses of quark and antiquark, placed at \vec{r}_1 and \vec{r}_2 , respectively. The static inter-quark potential $V^{(0)}(r \equiv |\vec{r}_1 - \vec{r}_2|)$ emerges, accompanied by relativistic corrections classified in powers of $1/m$. The potentials $V^{(1,0)}(r) = V^{(0,1)}(r) (\equiv V^{(1)}(r))$ are the corrections at $O(1/m)$. The potentials $V^{(2,0)}(r)$, $V^{(0,2)}(r)$, and $V^{(1,1)}(r)$ are the corrections at $O(1/m^2)$, which contain the leading order spin-dependent potentials [5, 6, 7] and the velocity-dependent potentials [8, 9]. Spin-dependent potentials are relevant to describing the fine and hyper-fine splitting of heavy quarkonium spectra. Once these potentials are determined, various properties of heavy quarkonium, not only the ground state but also excited states, e.g. full spectrum and wave functions, can be investigated systematically by solving the Schrödinger equation.

One may rely on perturbation theory to determine these potentials in the short-distance region. For instance, perturbative studies of the $O(1/m)$ potential yield $V^{(1)}(r) = -C_F C_A \alpha_s^2 / (4r^2)$ [10, 11, 2], where $C_F = 4/3$ and $C_A = 3$ are the Casimir charges of the fundamental and adjoint representations, respectively, and $\alpha_s = g^2 / (4\pi)$ the strong coupling (for the expression beyond leading-order perturbation theory, see [12]). However, since the binding energy of a quark and an antiquark is typically of the scale mv^2 , which can be of the same order as Λ_{QCD} due to the nonrelativistic nature of the system, $v \ll 1$, as well as the fact that perturbation theory cannot incorporate quark confinement, it is essential to determine the potentials nonperturbatively.

Monte Carlo simulations of lattice QCD offer a powerful tool for the nonperturbative determination of the potentials. The static potential can easily be determined from the expectation value of the $r \times t_w$ rectangular Wilson loop by $V^{(0)}(r) = -\lim_{t_w \rightarrow \infty} (1/t_w) \ln \langle W(r, t_w) \rangle$. The result is well parametrized by the Coulomb plus linear confining term,

$$V^{(0)}(r) = -\frac{c}{r} + \sigma r + \mu, \quad (1.2)$$

where c denotes the Coulombic coefficient, σ the string tension and μ a constant term. Recently, we investigated the $O(1/m)$ potential [13] and the $O(1/m^2)$ spin-dependent potentials [14, 15] on the lattice utilizing a new method, and obtained remarkably clean signals up to distances of around 0.6 fm. We then observed a certain deviation from the perturbative potentials at intermediate distances.

In this presentation we further investigate the relativistic corrections to the static potential. In particular, we aim to clarify the long-distance behavior of the $O(1/m)$ potential, and to determine the $O(1/m^2)$ velocity-dependent potentials. One attempt to determine the velocity dependent potentials on the lattice was published a decade ago [16], but the signal was lost due to large statistical errors.

2. Spectral representation of the $O(1/m)$ and $O(1/m^2)$ potentials

According to pNRQCD, the $O(1/m)$ and $O(1/m^2)$ potentials can generally be expressed by the *matrix elements* and the *energy gaps* of the spectral representation of the field strength correlators on the quark-antiquark source [2, 3].

Writing the eigenstate of the pNRQCD hamiltonian at $O(m^0)$ in the $\mathbf{3} \otimes \mathbf{3}^*$ representation of SU(3) color, which corresponds to the static quark-antiquark state, as $|n\rangle \equiv |n; \vec{r}_1, \vec{r}_2\rangle$, the correlator of two color-electric field strength operators $E^i = F_{4i}$ ($i = 1, 2, 3$), put on \vec{r}_a and \vec{r}_b ($a, b = 1, 2$) in space and separated $t = t_1 - t_2$ in time, takes the form

$$C(r, t) = \sum_{n=1}^{\infty} \langle 0 | gE^i(\vec{r}_a) | n \rangle \langle n | gE^j(\vec{r}_b) | 0 \rangle e^{-(\Delta E_{n0}(r))t}, \quad (2.1)$$

where $\Delta E_{n0}(r) \equiv E_n(r) - E_0(r)$ denotes the energy gap with $E_0(r) = V^{(0)}(r)$.

Then, the $O(1/m)$ potential is given by

$$V^{(1)}(r) = -\frac{1}{2} \delta_{ij} \sum_{n=1}^{\infty} \frac{\langle 0 | gE^i(\vec{r}_1) | n \rangle \langle n | gE^j(\vec{r}_1) | 0 \rangle}{(\Delta E_{n0}(r))^2}, \quad (2.2)$$

where two color-electric field strengths are attached to one of the quarks.

The spin-independent part of the $O(1/m^2)$ potential is written as

$$\begin{aligned} V_{\text{SI}}(r) = & \frac{1}{m_1^2} \left(\frac{1}{2} \{ \vec{p}_1^2, V_{p^2}^{(2,0)}(r) \} + \frac{1}{r^2} V_{l^2}^{(2,0)}(r) \vec{l}_1^2 + V_r^{(2,0)}(r) \right) \\ & + \frac{1}{m_2^2} \left(\frac{1}{2} \{ \vec{p}_1^2, V_{p^2}^{(0,2)}(r) \} + \frac{1}{r^2} V_{l^2}^{(0,2)}(r) \vec{l}_2^2 + V_r^{(0,2)}(r) \right) \\ & + \frac{1}{m_1 m_2} \left(-\frac{1}{2} \{ \vec{p}_1 \cdot \vec{p}_2, V_{p^2}^{(1,1)}(r) \} - \frac{1}{2r^2} V_{l^2}^{(1,1)}(r) (\vec{l}_1 \cdot \vec{l}_2 + \vec{l}_2 \cdot \vec{l}_1) + V_r^{(1,1)}(r) \right), \end{aligned} \quad (2.3)$$

where $\vec{l}_a = \vec{r} \times \vec{p}_a$. The functions specified by the subscripts p^2 and l^2 are related to the velocity-dependent potentials, V_b , V_c , V_d and V_e defined in Refs. [8, 9], by

$$\begin{aligned} V_{p^2}^{(2,0)}(r) &= V_{p^2}^{(0,2)}(r) = V_d(r) - \frac{2}{3} V_e(r), \quad V_{l^2}^{(2,0)}(r) = V_{l^2}^{(0,2)}(r) = V_e(r), \\ V_{p^2}^{(1,1)}(r) &= -V_b(r) + \frac{2}{3} V_c(r), \quad V_{l^2}^{(1,1)}(r) = -V_c(r), \end{aligned} \quad (2.4)$$

and then we have

$$V_b(r) = -\frac{2}{3} \delta_{ij} \sum_{n=1}^{\infty} \frac{\langle 0 | gE^i(\vec{r}_1) | n \rangle \langle n | gE^j(\vec{r}_2) | 0 \rangle}{(\Delta E_{n0})^3}, \quad (2.5)$$

$$V_c(r) = 3 \left(\frac{r_i r_j}{r^2} - \frac{\delta_{ij}}{3} \right) \sum_{n=1}^{\infty} \frac{\langle 0 | gE^i(\vec{r}_1) | n \rangle \langle n | gE^j(\vec{r}_2) | 0 \rangle}{(\Delta E_{n0})^3}, \quad (2.6)$$

$$V_d(r) = \frac{1}{3} \delta_{ij} \sum_{n=1}^{\infty} \frac{\langle 0 | gE^i(\vec{r}_1) | n \rangle \langle n | gE^j(\vec{r}_1) | 0 \rangle}{(\Delta E_{n0})^3}, \quad (2.7)$$

$$V_e(r) = -\frac{3}{2} \left(\frac{r_i r_j}{r^2} - \frac{\delta_{ij}}{3} \right) \sum_{n=1}^{\infty} \frac{\langle 0 | gE^i(\vec{r}_1) | n \rangle \langle n | gE^j(\vec{r}_1) | 0 \rangle}{(\Delta E_{n0})^3}. \quad (2.8)$$

For V_d and V_e two field strengths are attached to one of the quarks as for the $V^{(1)}$, while for V_b and V_c two field strengths are attached to the quark and the antiquark, respectively.

Thus, once the matrix elements and the energy gaps are known from the behavior of the field strength correlators on the quark-antiquark source, one can compute the potentials.

3. Numerical procedures

We work in Euclidean space in four dimensions on a hypercubic lattice with lattice volume $V = L^3 T$ and lattice spacing a , where we impose periodic boundary conditions in all directions. We use the Polyakov loop correlation function (PLCF, a pair of Polyakov loops P separated by a distance r) as the quark-antiquark source and evaluate the color-electric field strength correlators on the PLCF,

$$C(r, t) = \langle\langle gE^i(\vec{r}_a, t_1) gE^j(\vec{r}_b, t_2) \rangle\rangle_c = \langle\langle gE^i(\vec{r}_a, t_1) gE^j(\vec{r}_b, t_2) \rangle\rangle - \langle\langle gE^i(\vec{r}_a) \rangle\rangle \langle\langle gE^j(\vec{r}_b) \rangle\rangle, \quad (3.1)$$

using the multi-level algorithm [13, 15], where the double bracket represents the ratio of expectation values $\langle\langle \dots \rangle\rangle = \langle \dots \rangle_{PP^*} / \langle PP^*(r) \rangle$, while $\langle \dots \rangle_{PP^*}$ means that the color-electric field is connected to the Polyakov loop in a gauge invariant way. The subtracted term on the r.h.s. of Eq. (3.1) can be nonzero as the color-electric field is even under CP transformations. The spectral representation of Eq. (3.1) derived with transfer matrix theory reads [15]

$$C(r, t) = 2 \sum_{n=1}^{\infty} \langle 0 | gE^i(\vec{r}_a) | n \rangle \langle n | gE^j(\vec{r}_b) | 0 \rangle e^{-(\Delta E_{n0})T/2} \cosh((\Delta E_{n0})(\frac{T}{2} - t)) + O(e^{-(\Delta E_{10})T}), \quad (3.2)$$

where the last term represents terms of exponential factors equal to or smaller than $\exp(-(\Delta E_{10})T)$, which can be neglected for a reasonably large T . Thus, once Eq. (3.1) is evaluated via Monte Carlo simulations, we can fit the matrix element $\langle 0 | gE^i(\vec{r}_a) | n \rangle \langle n | gE^j(\vec{r}_b) | 0 \rangle$ and the energy gap ΔE_{n0} in Eq. (3.2), both of which are finally inserted into Eq. (2.2), etc. It is clear that Eq. (3.2) is reduced to the form like Eq. (2.1) in the infinite volume limit $T \rightarrow \infty$.

We define the lattice color-electric field operator, $ga^2 E^i(s)$, from the traceless part of $[U_{4i}(s) - U_{4i}^\dagger(s)]/(2i)$ with two-leaf modification (an average of $F_{4i}(s)$ and $F_{4i}(s - \hat{i})$), where $U_{\mu\nu}(s)$ is a plaquette variable defined on the site s . We multiply the Huntley-Michael factor [17] on the PLCF, Z_E [15], to the lattice color-electric field to cancel the self energies at least at $O(g^2)$.

We point out several advantages of our procedure which enable us to reduce numerical errors. In earlier studies of the relativistic corrections on the lattice, the Wilson loop has been used as the quark-antiquark source, since the corrections have been expressed as the integral of the field strength correlators on the Wilson loop with respect to the relative temporal distance between two field strength operators, t (see, e.g. [5]). They are, in principle, measurable on the lattice, and the result is reduced to Eq. (2.2) once the spectral decomposition is applied by using transfer matrix theory, and the temporal size of the Wilson loop is taken to infinity. In practice, however, the integration of the field strength correlator and the extrapolation of the temporal size of the Wilson loop to infinity cause systematic errors. In contrast, we can avoid these systematic errors once the field strength correlator is determined accurately, since we directly evaluate the matrix elements and the energy gaps. The use of the PLCF as the quark-antiquark source and its spectral representation

allows us to take into account the finite- T effect automatically in the fit. We should note however that if one uses the commonly employed simulation algorithms, it is almost impossible to evaluate the field strength correlators on the PLCF, or the PLCF itself, at intermediate distances with reasonable computational effort, since the expectation value of the PLCF at zero temperature is smaller by several orders of magnitude than that of the Wilson loop. However this problem is solved by employing the multi-level algorithm [18]. For details of our implementation, see [15].

4. Numerical results

We carry out simulations using the standard Wilson gauge action in SU(3) lattice gauge theory. We summarize our simulation parameters in Table 1. The lattice spacing a is set from the Sommer scale $r_0 = 0.5$ fm. For a reference we compute the static potential and the force from the PLCF,

$$V^{(0)}(r) = -\frac{1}{T} \ln \langle PP^*(r) \rangle + O(e^{-(\Delta E_{10})T}), \quad \frac{dV^{(0)}(r)}{dr} = \frac{V^{(0)}(r) - V^{(0)}(r-a)}{a}, \quad (4.1)$$

which are shown in Fig. 1. The fitting of the potential data at $\beta = 6.00$ to the functional form in Eq. (1.2) yields $c = 0.2808(5)$, $\sigma a^2 = 0.0468(1)$ and $\mu a = 0.7301(4)$ with $\chi^2/N_{\text{df}} = 3.5$. We note that the large value of χ^2/N_{df} just reflects the fact that the Coulombic coefficient is not strictly constant as a function of r , which will be clear once the second derivative of the potential is investigated [18, 15], but we ignore this effect for the moment.

Table 1: Simulation parameters used in this study. N_{tsl} is the number of time slices in a sublattice and N_{iupd} the number of internal update within a sublattice, both are parameters for the multi-level algorithm.

$\beta = 6/g^2$	a [fm]	$(L/a)^3(T/a)$	N_{tsl}	N_{iupd}	N_{conf}
5.85	0.123	$18^3 24$	3	50000	100
6.00	0.093	$24^3 32$	4	50000	45

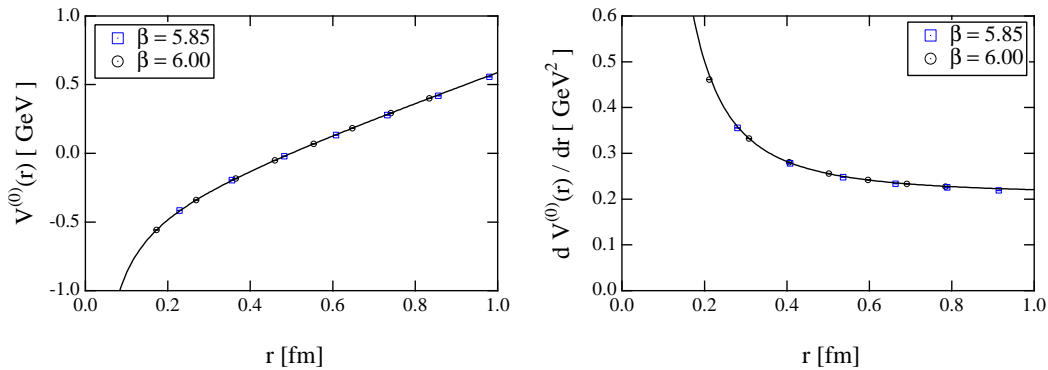


Figure 1: Static potential $V^{(0)}(r)$ and the force $dV^{(0)}(r)/dr$ as a function of r , which is improved with treelevel perturbation theory. The potentials of different β values are normalized at $r = 0.5$ fm.

In Fig. 2, we show the typical behavior of the longitudinal and the transverse components of the color-electric field strength correlators, where the quark-antiquark axis has been taken along the

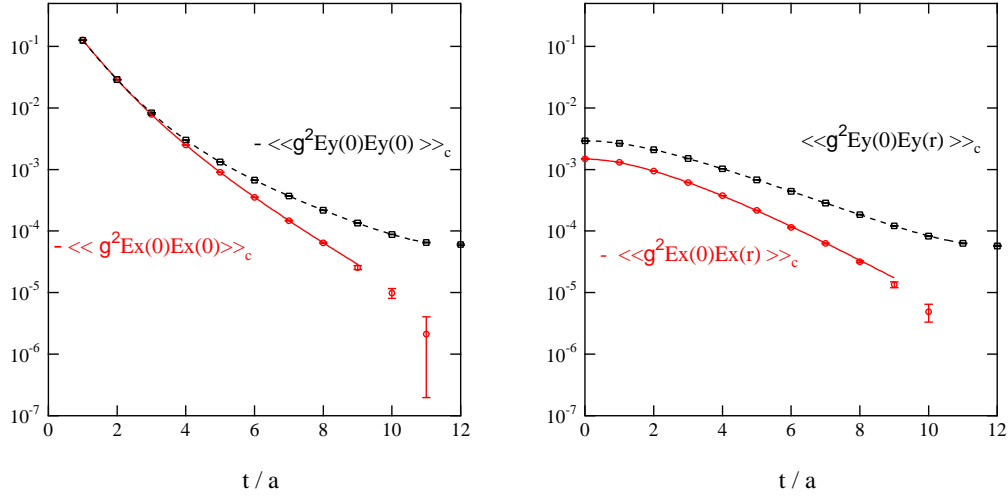


Figure 2: Color-electric field strength correlators at $\beta = 5.85$ on the $18^3 24$ lattice for $r/a = 5$.

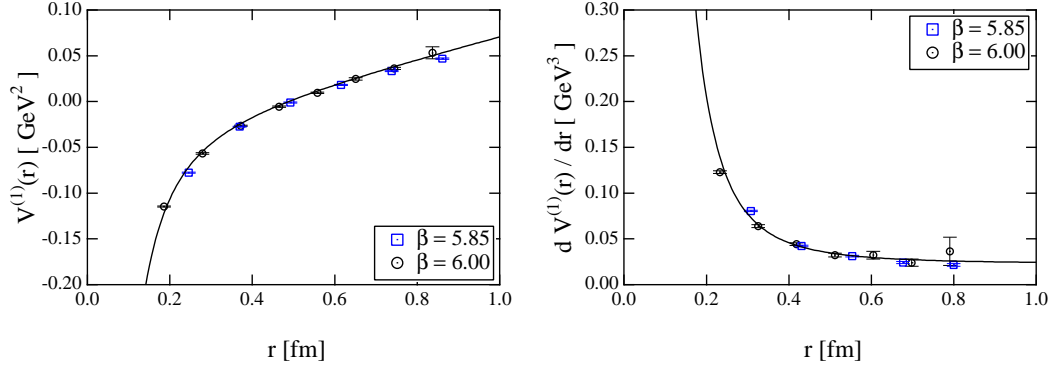


Figure 3: The $O(1/m)$ potential and the force.

x axis. We select the data at $r/a = 5$, $\beta = 5.85$ as an example. Statistical errors of the correlators are small enough to determine the matrix elements and the energy gaps with the fit based on Eq. (3.2). It is evident that Eq. (3.2) describes the data very well. Here, since it is impossible to determine the matrix elements and the energy gaps for all $n \geq 1$ with the limited data points, we truncated expansion in Eq. (3.2) at a certain $n = n_{\max}$. The validity of the truncation was monitored by looking at the reduced χ^2 defined with the full covariance matrix. In all cases we found that $n_{\max} = 3$ gave the best result.

We then computed the $O(1/m)$ potential and the $O(1/m^2)$ velocity-dependent potentials, which are plotted in Figs. 3 and 4, respectively. Note that each potential contains a constant contribution, which depends on β . Here we normalized the potentials at $r = 0.5$ fm by assuming perfect scaling behavior. This assumption is justified at intermediate distance, where the data at different lattice spacings fall into a smooth curve. Small discrepancies at short distances, however, cannot be avoided in the present simulation. The data at short distances are sensitive to the way of discretization and the definition of the renormalized color-electric field operator.

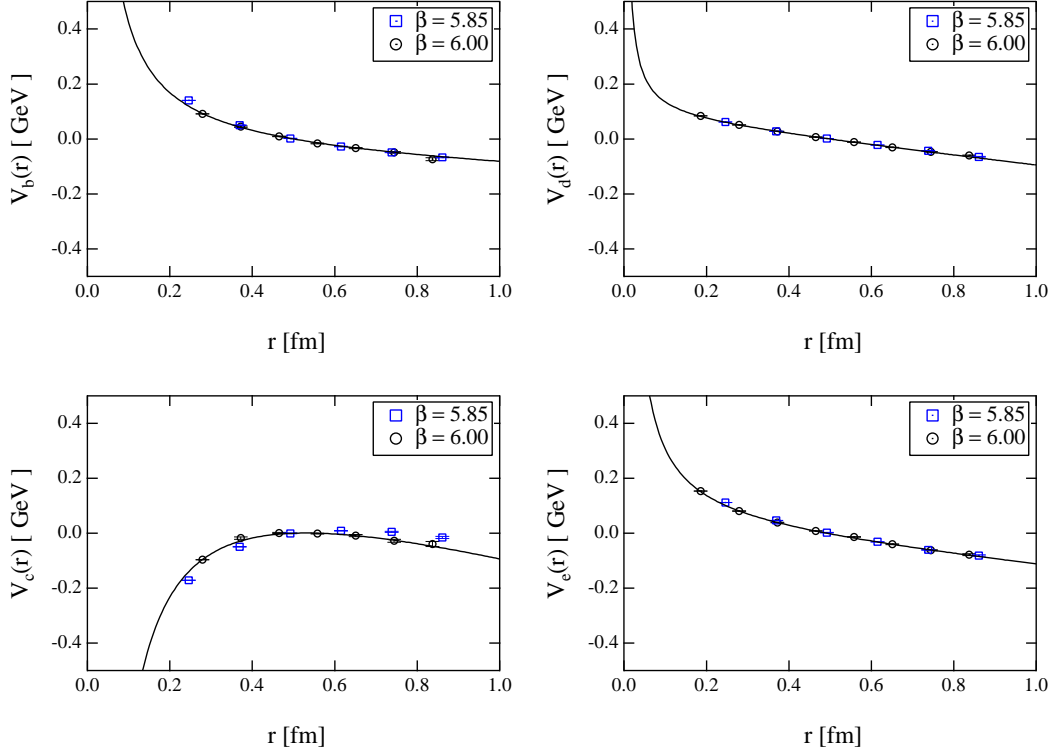


Figure 4: The $O(1/m^2)$ velocity-dependent potentials.

The functional form of the $O(1/m)$ potential is not yet established nonperturbatively. In our previous study [13], we found that a $1/r$ function describes the data well, but this result was valid only up to $r = 0.6$ fm. Now we have further long distance data up to distances of $r = 0.9$ fm. We empirically examined various functional forms and found that, if we include the data $r > 0.6$ fm, the $1/r$ function is not supported by the fit, while the perturbative $1/r^2$ function with the linear term can fit the data well. Using the functional form

$$V_{\text{fit}}^{(1)}(r) = -\frac{c'}{r^2} + \sigma' r + \mu', \quad (4.2)$$

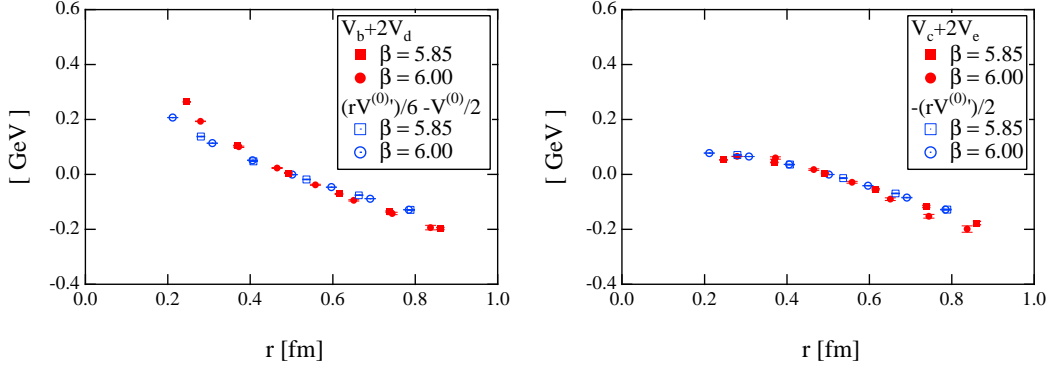
we obtain $c' = 0.090(5)$, $\sigma' a^3 = 0.0024(1)$, and $\mu' a^2 = 0.389(1)$ with $\chi^2/N_{\text{df}} = 0.68$ for the data at $\beta = 6.00$, where the distance $r/a = 2$ is omitted. In Fig. 3, we also plot the force of the $O(1/m)$ potential defined by $\frac{dV_{\text{fit}}^{(1)}(r)}{dr} = (V^{(1)}(r) - V^{(1)}(r-a))/a$. We find that the fit of the force to the function $\frac{dV_{\text{fit}}^{(1)}(r)}{dr} = \frac{2c'}{r^3} + \sigma'$ gives $c' = 0.095(5)$, $\sigma' = 0.0024(1)$ with $\chi^2/N_{\text{df}} = 0.62$, which is consistent with the fit result of the potential.

By taking into account the masses $(1/m_1 + 1/m_2)$ in Eq. (1.1), we may estimate the correction to the string tension in the static potential. For charmonium, $m_c = 1.3$ GeV, we find $(2/m_c)\sigma' = 0.179$ GeV/fm, which is compared to $\sigma = 1.07(1)$ GeV/fm. The correction is about 17 %. For bottomonium, $m_b = 4.7$ GeV, we find $(2/m_b)\sigma' = 0.049$ GeV/fm, so that the correction is about 5 %.

Next, we may characterize the functional form of the velocity-dependent potentials. Here, motivated by the minimal area law (MAL) model [8, 9], we fit the potentials to the same functional

Table 2: Fit result of the velocity dependent potential to the function $V_{\text{fit}}(r) = -c/r + \sigma r + \mu$.

	c	σa^2	μa	χ^2/N_{df}
V_b	-0.25(2)	-0.003(1)	-0.08(1)	1.5
V_c	0.61(4)	-0.019(2)	0.08(2)	3.0
V_d	-0.042(4)	-0.0076(3)	-0.187(2)	4.3
V_e	-0.156(4)	-0.0069(3)	-0.017(2)	4.6


Figure 5: Test of the BBMP relations in Eq. (4.3).

form as the static potential. Again, we omit the point at $r/a = 2$ from the analysis of the data taken at $\beta = 6.00$. The fitting results are summarized in Table 2. The global structure of the data seems to be well described by the fitting function as seen in Fig. 4, though χ^2/N_{df} may be relatively large.

Finally we examine some nonperturbative relations which connect the velocity-dependent potentials to the static potential [8, 9], which are often called the BBMP relations,

$$V_b(r) + 2V_d(r) = -\frac{1}{2}V^{(0)}(r) + \frac{r}{6} \frac{dV^{(0)}(r)}{dr}, \quad V_c(r) + 2V_e(r) = -\frac{r}{2} \frac{dV^{(0)}(r)}{dr}. \quad (4.3)$$

These relations are derived by exploiting the exact Poincaré invariance of the field strength correlator, and hence one expects corrections due to lattice artifacts, which would vanish in the continuum limit. These relations can be regarded as an extension of the Gromes relation [19] for the $O(1/m^2)$ spin-dependent potentials. In Fig. 5, we show the result, where the constant contribution of the potentials is normalized at $r = 0.5$ fm. The BBMP relations seem to be satisfied, though we see a small discrepancy especially at short distances.

5. Summary

We have investigated the relativistic corrections to the static potential, the $O(1/m)$ potential and the $O(1/m^2)$ velocity-dependent potentials, in SU(3) lattice gauge theory. They are important ingredients of the pNRQCD hamiltonian for heavy quarkonium.

By evaluating the color-electric field strength correlator on the PLCF with the multi-level algorithm, and exploiting the spectral representation of the correlator, we have obtained a very clean signal for these potentials up to $r = 0.9$ fm. The $O(1/m)$ potential contains a linearly rising

nonperturbative contribution. The $O(1/m^2)$ velocity-dependent potentials are non-vanishing at long distances.

All potentials at different β values, normalized at $r = 0.5$ fm, show a reasonable scaling behavior. The BBMP relations are apparently satisfied around $r \simeq 0.5$ fm. Although we have applied the Huntley-Michael prescription in the present study to remove the self-energy contributions of the field strength operator, a more systematic, non-perturbative renormalization procedure of field strength operators is highly desirable. Since the statistical errors of the potentials are reduced significantly owing to the multi-level algorithm, we now face such a delicate problem.

The comparison with various models [9, 20] and phenomenology [21, 22, 23] are of course to be done. In particular, it is quite interesting to examine the effect of the $O(1/m)$ potential on the spectrum as this is the leading-order relativistic correction in the $1/m$ expansion.

Acknowledgments

The main calculation has been performed on the NEC-SX8 at Research Center for Nuclear Physics (RCNP), Osaka University, Japan.

References

- [1] N. Brambilla, A. Pineda, J. Soto, and A. Vairo, *Potential NRQCD: An effective theory for heavy quarkonium*, Nucl. Phys. **B566** (2000) 275 [hep-ph/9907240].
- [2] N. Brambilla, A. Pineda, J. Soto, and A. Vairo, *The QCD potential at $O(1/m)$* , Phys. Rev. **D63** (2001) 014023 [hep-ph/0002250].
- [3] A. Pineda and A. Vairo, *The QCD potential at $O(1/m^2)$: Complete spin-dependent and spin-independent result*, Phys. Rev. **D63** (2001) 054007 [hep-ph/0009145], Erratum-*ibid* **D64** (2001) 039902.
- [4] N. Brambilla, A. Pineda, J. Soto, and A. Vairo, *Effective field theories for heavy quarkonium*, Rev. Mod. Phys. **77** (2005) 1423 [hep-ph/0410047].
- [5] E. Eichten and F. Feinberg, *Spin dependent forces in heavy quark systems*, Phys. Rev. Lett. **43** (1979) 1205.
- [6] E. Eichten and F. Feinberg, *Spin dependent forces in QCD*, Phys. Rev. **D23** (1981) 2724.
- [7] D. Gromes, *Relativistic corrections to the long range quark anti-quark potential, electric flux tubes, and area law*, Z. Phys. **C22** (1984) 265.
- [8] A. Barchielli, E. Montaldi, and G.M. Prosperi, *On a systematic derivation of the quark-antiquark potential*, Nucl. Phys. **B296** (1988) 625, Erratum-*ibid* **B303** (1988) 752.
- [9] A. Barchielli, N. Brambilla, and G.M. Prosperi, *Relativistic corrections to the quark-antiquark potential and the quarkonium spectrum*, Nuovo Cim. **A103** (1990) 59.
- [10] K. Melnikov and A. Yelkhovsky, *Top quark production at threshold with $O(\alpha_s^2)$ accuracy*, Nucl. Phys. **B528** (1998) 59 [hep-ph/9802379].
- [11] A.H. Hoang, *Bottom quark mass from Upsilon mesons*, Phys. Rev. **D59** (1999) 014039 [hep-ph/9803454].
- [12] N. Brambilla, A. Pineda, J. Soto, and A. Vairo, *The heavy quarkonium spectrum at order $m\alpha_s^5 \ln \alpha_s$* , Phys. Lett. **B470** (1999) 215 [hep-ph/9910238].

- [13] Y. Koma, M. Koma, and H. Wittig, *Nonperturbative determination of the QCD potential at $O(1/m)$* , Phys. Rev. Lett. **97** (2006) 122003 [hep-lat/0607009].
- [14] M. Koma, Y. Koma, and H. Wittig, *Determination of the spin-dependent potentials with the multi-level algorithm*, PoS **LAT2005** (2005) 216 [hep-lat/0510059].
- [15] Y. Koma and M. Koma, *Spin-dependent potentials from lattice QCD*, Nucl. Phys. **B769** (2007) 79 [hep-lat/0609078].
- [16] G.S. Bali, K. Schilling, and A. Wachter, *Complete $O(v^2)$ corrections to the static interquark potential from $SU(3)$ gauge theory*, Phys. Rev. **D56** (1997) 2566 [hep-lat/9703019].
- [17] A. Huntley and C. Michael, *Spin-spin and spin-orbit potentials from lattice gauge theory*, Nucl. Phys. **B286** (1987) 211.
- [18] M. Lüscher and P. Weisz, *Quark confinement and the bosonic string*, JHEP **07** (2002) 049 [hep-lat/0207003].
- [19] D. Gromes, *Spin dependent potentials in QCD and the correct long range spin orbit term*, Z. Phys. **C26** (1984) 401.
- [20] N. Brambilla and A. Vairo, *Heavy quarkonia: Wilson area law, stochastic vacuum model and dual QCD*, Phys. Rev. **D55** (1997) 3974 [hep-ph/9606344].
- [21] D. Ebert, V.O. Galkin, and R.N. Faustov, *Mass spectrum of orbitally and radially excited heavy-light mesons in the relativistic quark model*, Phys. Rev. **D57** (1998) 5663 [hep-ph/9712318].
- [22] D. Ebert, R.N. Faustov, and V.O. Galkin, *Quark-antiquark potential with retardation and radiative contributions and the heavy quarkonium mass spectra*, Phys. Rev. **D62** (2000) 034014 [hep-ph/9911283].
- [23] D. Ebert, R.N. Faustov, and V.O. Galkin, *Properties of heavy quarkonia and B_c mesons in the relativistic quark model*, Phys. Rev. **D67** (2003) 014027 [hep-ph/0210381].